PERGAMON

International Journal of Multiphase Flow 26 (2000) 1621–1644

International Journal of Multiphase Flow

www.elsevier.com/locate/ijmulflow

Linear analysis of the temporal instability of axisymmetrical non-Newtonian liquid jets

Günter Brenn*, Zhengbai Liu, Franz Durst

Lehrstuhl für Strömungsmechanik, University of Erlangen-Nürnberg, Cauerstrasse 4, 91058 Erlangen, Germany

Received 10 February 1998; received in revised form 23 November 1999

Abstract

The temporal instability behavior of non-Newtonian liquid jets moving in an inviscid gaseous environment is investigated theoretically for axisymmetrical disturbances. The corresponding dispersion relation between the wave growth rate and the wave number is derived. The linearized stability analysis shows that a jet of a viscoelastic fluid exhibits a larger growth rate of axisymmetric disturbances than a jet of a Newtonian fluid with the same Ohnesorge number, indicating that non-Newtonian liquid jets are more unstable than their Newtonian counterparts. This is a well-known effect for small perturbations of the jet surface. For non-Newtonian liquid jets the instability behavior is influenced by the interaction of the liquid viscosity and elasticity effects, in which the liquid viscosity tends to dampen the instability, whereas the elasticity results in an enhancement of instability for small perturbations. The validity of the theoretical results for the growth rate spectra and breakup lengths of viscoelastic liquid jets is tested against experimental results from the literature. The comparisons confirm that the linearized theory fails to describe the nonlinear phenomena involved in viscoelastic jet breakup correctly, but it yields good results for the growth rate of disturbances in a regime of low jet Weber numbers and small deformations. The limits of validity of linear theories for viscoelastic jet instability are quantified, taking also into account the onset of non-axisymmetric deformations due to bending.

Keywords: Temporal instability; Non-Newtonian liquid jets; Axisymmetrical disturbances; Linear analysis

1. Introduction

The instability and atomization of an axisymmetric liquid jet issuing from a nozzle is involved in many practical applications such as in fuel atomization, spray coating, spray

* Corresponding author. Fax: +49-9131-8529503.

0301-9322/00/$ - see front matter
PII: S0301-9322(99)00115-9

drying, pesticide spraying and many others. Since in many of these processes non-Newtonian liquids may be involved, it is of interest and importance to understand the mechanisms of instability and breakup of jets of such liquids, since the efficiency and quality of production is strongly dependent on the details of this physical phenomenon.

The capillary instability of axisymmetric liquid jets has been the subject of numerous experimental and theoretical investigations since the 19th century. Rayleigh (1878, 1879) considered the capillary instability of a cylinder of an inviscid fluid in a vacuum, and he also discussed the case of a viscous liquid jet without inertia (Rayleigh, 1892). Weber (1931) obtained the complete linear solution for a viscous Newtonian liquid jet under surface tension forces in which he also included the action of an inviscid atmosphere. Tomotika (1935) extended the solution to include the effect of a viscous surrounding. Even today, the analytical solutions from the above pioneer works are often applied for the theoretical solution of practical problems.

Since then, more experimental and theoretical investigations on the mechanisms of liquid jet instability have been performed, e.g. by Middleman (1965), Kroesser and Middleman (1969), Yuen (1968), Goedde and Yuen (1970), McCarthy and Molloy (1974), Bogy (1979) and Chigier and Reitz (1996), and different theories have been proposed to explain the liquid jet instability behavior. The aerodynamic interaction between the liquid jet and the ambient gas is the most developed of the jet disintegration theories. It shows that the instability is enhanced by aerodynamic interaction between the liquid and the ambient gas which enhances unstable wave growth on the liquid surface. The growth of these unstable waves eventually breaks the liquid jet into ligaments, and then into drops (Li, 1995). Grant and Middleman (1966), Phinney (1973) and Sterling and Sleicher (1975) showed that the effect of air moves the most rapidly growing mode to the shortwave part of the spectrum, i.e. the wavenumber at which the largest disturbance growth rate occurs increases due to the action of air. Using the predicted values of the growth rate, Sterling and Sleicher (1975) could describe the experimental curve $L = L(\bar{U})$ (L is the intact jet length and $\bar{U}$ is the jet velocity) around the maximum where the effect of air flow was assumed to become important. In order to achieve this agreement, the theory assuming a plug flow in the jet was modified empirically in order to account for velocity profile relaxation effects. The modification consisted in the multiplication of the aerodynamic force term with a factor $C = 0.175$. The applicability of a similar theory to viscoelastic jets has not been checked in the literature by date.

So far, considerable literature is available on liquid jet instability which is helpful to understand the mechanisms of the instability and breakup of liquid jets for Newtonian fluids (e.g. Middleman, 1965; Kroesser and Middleman, 1969; Goldin et al., 1969; Goren and Gottlieb, 1982). The instability and breakup mechanisms of non-Newtonian liquid jets have been treated in detail by Yarin (1993). For viscoelastic fluids the initial growth of disturbances with small amplitudes is enhanced as compared to Newtonian jets with the same Ohnesorge number. With increasing deformation, however, the non-Newtonian liquid behavior leads to a retardation of breakup and to the formation of a structure of drops connected by thin filaments (the so-called beads-on-string structure). This mechanism slows down the breakup of the jet considerably and leads to very large breakup lengths, despite the initially enhanced disturbance growth rates. The nonlinear solution for this type of jet breakup has been obtained by Yarin (1993). Goren and Gottlieb (1982) showed that the onset of this effect may be

described by a linear analysis when an unrelaxed axial tension is included in the momentum equation. This leads to an additional term in the dispersion relation which depends on a non-dimensional elastic tension group. It is well known that the whole mechanism of viscoelastic jet breakup is highly nonlinear. Therefore, it is quite obvious that linear theories are not capable to describe this phenomenon correctly.

The objective of the present work is to derive a dispersion relation from a linear stability analysis for non-Newtonian liquid jets under the action of surface tension and aerodynamic forces, to test its restriction in describing the real effects in non-Newtonian liquid jet breakup, and to analyze its predictions of the jet behavior. It is well known that linearized theories cannot describe the nonlinear stabilizing behavior of, e.g., viscoelastic liquids at the stage of strong deformations before jet breakup. The degree of failure of the linearized theory in describing the jet breakup length is quantified. The onset of instability phenomena like bending, which produces non-axisymmetric jet deformations at sufficiently high jet Weber numbers and can therefore also not be described by the present theory, is considered using the onset criterion established in Yarin (1993).

In the following section, the dispersion relation between the growth rate of disturbance waves and the wave number is derived for a non-Newtonian liquid jet injected into an inviscid gaseous medium. Then, the predictions of the derived equation are investigated in comparison with theoretical and experimental results from the literature. A further section is devoted to the analysis of the derived equation. Conclusions are drawn in Section 4.

2. Theory

We consider an axisymmetric jet of a non-Newtonian liquid of density ρ, surface tension σ, and radius a moving with velocity $\bar{U}$ through an inviscid gas of density ρ_G. Owing to the axisymmetry of the problem, i.e., the jet cross section remains circular and contracts or expands, the governing equations are written in a cylindrical coordinate system for convenience. The coordinates are chosen such that the z axis is parallel to the moving direction of the liquid jet flow, and the r axis is normal to the liquid jet with its origin located at the axis of symmetry. Fig. 1 shows a schematic diagram of the liquid jet and the coordinate system. The analysis of the present problem was given in the literature by many authors before. Therefore, it is not repeated in full detail here. Only a sketch of the derivations together with the final result is presented in the following sections.

2.1. Liquid phase velocity and pressure distribution

The governing equations of the liquid motion in a jet are the conservation laws of mass and momentum, as given below:

$$\frac{\partial \rho}{\partial t} + \nabla \cdot \rho \mathbf{v} = 0 \tag{1}$$

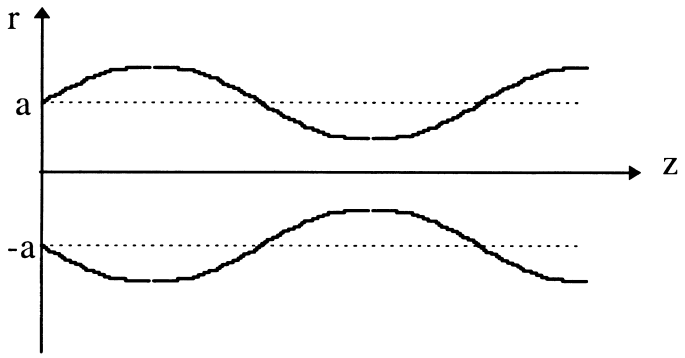

Fig. 1. Schematic diagram of a liquid jet with axisymmetrical surface disturbances and the laboratory-fixed coordinate system r, z.

$$\left(\frac{\partial}{\partial t}+\mathbf{v}\cdot\nabla\right)\rho\mathbf{v}=-\nabla\cdot\boldsymbol{\pi}+\rho\mathbf{g} \tag{2}$$

where t is time, $\mathbf{v}$ is the liquid velocity vector, $\mathbf{g}$ is the gravitational acceleration vector, and $\boldsymbol{\pi}$ is the total stress tensor of the liquid, which is given by

$$\boldsymbol{\pi}=p\boldsymbol{\delta}+\boldsymbol{\tau} \tag{3}$$

where p is the pressure of the liquid due to the disturbance, $\boldsymbol{\tau}$ is the extra stress tensor of the liquid, and $\boldsymbol{\delta}$ is the unit tensor.

The corotational Oldroyd eight-constant model is used for describing the viscoelastic liquid state, which has the following general constitutive equation in the objective reference frames (Bird et al., 1977; Park and Lee, 1995; Goren and Gottlieb, 1982; Liu et al., 1998)

$$\begin{aligned}&\boldsymbol{\tau}+\lambda_1\frac{\mathrm{D}\boldsymbol{\tau}}{\mathrm{D}t}+\frac{1}{2}\mu_0(\mathrm{tr}\,\boldsymbol{\tau})\dot{\boldsymbol{\gamma}}-\frac{1}{2}\mu_1\{\boldsymbol{\tau}\cdot\dot{\boldsymbol{\gamma}}+\dot{\boldsymbol{\gamma}}\cdot\boldsymbol{\tau}\}+\frac{1}{2}\nu_1(\boldsymbol{\tau}:\dot{\boldsymbol{\gamma}})\boldsymbol{\delta}\\&\quad=-\eta_0\left[\dot{\boldsymbol{\gamma}}+\lambda_2\frac{\mathrm{D}\dot{\boldsymbol{\gamma}}}{\mathrm{D}t}-\mu_2\{\dot{\boldsymbol{\gamma}}\cdot\dot{\boldsymbol{\gamma}}\}+\frac{1}{2}\nu_2(\dot{\boldsymbol{\gamma}}:\dot{\boldsymbol{\gamma}})\boldsymbol{\delta}\right]\end{aligned} \tag{4}$$

where

$$\dot{\boldsymbol{\gamma}}=\nabla\mathbf{v}+(\nabla\mathbf{v})^{\mathrm{T}} \tag{5}$$

$$\boldsymbol{\omega}=\nabla\mathbf{v}-(\nabla\mathbf{v})^{\mathrm{T}} \tag{6}$$

$$\frac{\mathrm{D}\boldsymbol{\tau}}{\mathrm{D}t}=\frac{\partial\boldsymbol{\tau}}{\partial t}+(\mathbf{v}\cdot\nabla)\boldsymbol{\tau}+\frac{1}{2}\{\boldsymbol{\omega}\cdot\boldsymbol{\tau}-\boldsymbol{\tau}\cdot\boldsymbol{\omega}\} \tag{7}$$

$$\frac{\mathrm{D}\dot{\boldsymbol{\gamma}}}{\mathrm{D}t}=\frac{\partial\dot{\boldsymbol{\gamma}}}{\partial t}+(\mathbf{v}\cdot\nabla)\dot{\boldsymbol{\gamma}}+\frac{1}{2}\{\boldsymbol{\omega}\cdot\dot{\boldsymbol{\gamma}}-\dot{\boldsymbol{\gamma}}\cdot\boldsymbol{\omega}\} \tag{8}$$

In these equations, $\dot{\boldsymbol{\gamma}}$ is the rate of strain tensor, $\boldsymbol{\omega}$ is the vorticity tensor, D/Dt is defined as the corotational derivative, η_0 is the zero shear viscosity, λ_1 is the stress relaxation time, and λ_2 is the deformation retardation time of the liquid. The quantities μ_0, μ_1, μ_2, ν_1, and ν_2 are time constants of the model. Since the velocity of the liquid is small compared to the sound velocity, it is assumed that the liquid is incompressible. The following linearized equations are obtained after neglecting the nonlinear terms and gravitational effects:

$$\nabla \cdot \mathbf{v} = 0 \tag{9}$$

$$\rho\left(\frac{\partial}{\partial t} + \bar{U}\frac{\partial}{\partial x}\right)\mathbf{v} = -\nabla \cdot (p\boldsymbol{\delta} + \boldsymbol{\tau}) \tag{10}$$

$$\boldsymbol{\tau} + \lambda_1\left(\frac{\partial}{\partial t} + \bar{U}\frac{\partial}{\partial x}\right)\boldsymbol{\tau} = -\eta_0\left[\dot{\boldsymbol{\gamma}} + \lambda_2\left(\frac{\partial}{\partial t} + \bar{U}\frac{\partial}{\partial x}\right)\dot{\boldsymbol{\gamma}}\right]. \tag{11}$$

As the jet issues from the nozzle, the jet surface is subject to disturbances. The equation for the jet surface displaced by a small disturbance is expressed as follows:

$$r = a + \xi \tag{12}$$

where $r = a$ is the equilibrium position of the jet surface, i.e., the position without disturbances, and ξ is the displacement of a point on the surface.

The flow field solutions of the above governing equations must satisfy the kinematic and dynamic boundary conditions at the gas–liquid interface, which can be taken at $r = a$ (the first-order approximation for a small displacement of the interface due to the disturbance). Thus, in mathematical form, the kinematic boundary condition requires that

$$v_r = \left(\frac{\partial}{\partial t} + \bar{U} \cdot \nabla\right)\xi \tag{13}$$

and the dynamic boundary conditions require that

$$(\boldsymbol{\pi} - \boldsymbol{\pi}_{\mathrm{G}}) \times \mathbf{n} = 0 \tag{14}$$

$$(\boldsymbol{\pi} - \boldsymbol{\pi}_{\mathrm{G}}) \cdot \mathbf{n} + \sigma\nabla \cdot \mathbf{n} = 0 \tag{15}$$

where subscript G denotes the gas phase, σ is the surface tension, and $\mathbf{n}$ is the unit vector normal to the gas–liquid interface, pointing into the gas phase. These conditions can be linearized in the same manner as the governing equations. They are, to first order,

$$v_r = \frac{\partial \xi}{\partial t} + \bar{U}\frac{\partial \xi}{\partial z} \quad r = a \tag{16}$$

$$\pi_{rz} = \tau_{rz} = -\eta(\alpha)\left(\frac{\partial v_z}{\partial r} + \frac{\partial v_r}{\partial z}\right) = 0 \quad r = a \tag{17}$$

$$\pi_{rr} - \pi_{G,\,rr} + p_\sigma = 0 \quad r = a \tag{18}$$

where π_{rr} is the liquid normal stress, $\pi_{G,\,rr}$ is the gas normal stress, and p_σ is the pressure induced by the surface tension. Moreover, the velocity components along the jet axis, i.e., at, $r = 0$ must be finite.

When the jet is perturbed by symmetric disturbances, there is no motion of the liquid around the axis of symmetry, i.e., the velocity component in azimuthal direction $v_\theta = 0$ (Levich, 1962). However, v_θ may be nonzero in an axisymmetric system due to swirl. In the present study, swirl is not considered. Thus, the velocity vector $\mathbf{v}$ has only two components, that is:

$$\mathbf{v} = \mathbf{v}(r, z, t) = \left[v_r(r, z, t), v_z(r, z, t), 0\right] \tag{19}$$

Since we are interested in wave motion in the liquid, we seek the solutions for the velocity vector $\mathbf{v}$ as periodic functions in z, and complex exponential functions in t:

$$\mathbf{v} = \mathbf{V}(r)\mathrm{e}^{ikz+\alpha t} \tag{20}$$

where k is the wave number of the disturbance in z direction, and α is a complex frequency ($\alpha = \alpha_r + i\alpha_i$, where α_r represents the growth rate of the disturbance, α_i is 2π times the disturbance frequency, and $-\alpha_i/k$ is the wave propagation velocity of the disturbance, which may be due to aerodynamic forces directed along the jet). Thus, the stress tensor $\boldsymbol{\tau}$, the rate of strain tensor $\dot{\boldsymbol{\gamma}}$, the pressure p, and the interface displacement ξ are periodic functions in z, and exponential functions in t. They are formulated as

$$\boldsymbol{\tau} = \boldsymbol{T}(r)\mathrm{e}^{ikz+\alpha t} \tag{21}$$

$$\dot{\boldsymbol{\gamma}} = \dot{\boldsymbol{\Gamma}}(r)\mathrm{e}^{ikz+\alpha t} \tag{22}$$

$$p = P(r)\mathrm{e}^{ikz+\alpha t} \tag{23}$$

$$\xi = \xi_0\mathrm{e}^{ikz+\alpha t} \tag{24}$$

where ξ_0 is the initial amplitude of the disturbance, which is taken to be much smaller than the radius a of the jet.

Substitution of the above functions (21)–(24) into the equations of motion yields ordinary differential equations for the amplitude functions which are dependent on the radial coordinate only. Application of the boundary conditions allows for the calculation of the integration constants which appear in the solutions of these differential equations. The final forms of the velocity and pressure profiles in the liquid jet read

$$v_r = \left[\frac{l^2 + k^2}{I_1(ka)} I_1(kr) - \frac{2k^2}{I_1(la)} I_1(lr)\right] \frac{\eta(\alpha)}{\rho} \xi_0 \mathrm{e}^{ikz+\alpha t} \quad r \le a \tag{25}$$

$$v_z = i\left[\frac{l^2+k^2}{I_1(ka)}I_0(kr) - \frac{2kl}{I_1(la)}I_0(lr)\right]\frac{\eta(\alpha)}{\rho}\xi_0 e^{ikz+\alpha t} \quad r \le a \tag{26}$$

$$p = -\frac{l^2+k^2}{kI_1(ka)}I_0(kr)\eta(\alpha)\left(\alpha + ik\bar{U}\right)\xi_0 e^{ikz+\alpha t} \quad r \le a \tag{27}$$

where

$$l^2 = k^2 + \frac{\rho\left(\alpha + ik\bar{U}\right)}{\eta(\alpha)} \tag{28}$$

and

$$\eta(\alpha) = \eta_0\frac{1+\lambda_2\left(\alpha + ik\bar{U}\right)}{1+\lambda_1\left(\alpha + ik\bar{U}\right)} \tag{29}$$

2.2. Gas phase velocity and pressure distribution

In the present analysis, the gas around the moving liquid jet is assumed to be inviscid and incompressible, and it moves at a velocity $\bar{U}_G$ in the same direction as the flow of the liquid jet. Similar to the liquid phase, the governing equations for the gas phase are expressed in a linearized form as follows:

$$\frac{1}{r}\frac{\partial}{\partial r}(rv_{r,\,G}) + \frac{\partial v_{z,\,G}}{\partial z} = 0 \tag{30}$$

$$\rho_G\left(\frac{\partial v_{r,\,G}}{\partial t} + \bar{U}_G\frac{\partial v_{r,\,G}}{\partial z}\right) = -\frac{\partial p_G}{\partial r} \tag{31}$$

$$\rho_G\left(\frac{\partial v_{z,\,G}}{\partial t} + \bar{U}_G\frac{\partial v_{z,\,G}}{\partial z}\right) = -\frac{\partial p_G}{\partial z} \tag{32}$$

where Eq. (30) is the gas phase continuity equation, and Eqs. (31) and (32) are the gas phase momentum equations. The linearized boundary conditions for the gas phase are

$$v_{r,\,G} = \frac{\partial \xi}{\partial t} + \bar{U}_G\frac{\partial \xi}{\partial z} \quad r = a \tag{33}$$

$$v_{r,\,G} = 0 \quad r \to \infty \tag{34}$$

Similar to the governing differential equations for the liquid phase, the solutions for the velocity and pressure profiles in the gas phase are sought in the following form:

$$v_{r,\,G} = V_{r,\,G}(r)e^{ikz+\alpha t} \tag{35}$$

$$v_{z,\,\mathrm{G}} = V_{z,\,\mathrm{G}}(r)\mathrm{e}^{ikz+\alpha t} \tag{36}$$

$$p_{\mathrm{G}} = P_{\mathrm{G}}(r)\mathrm{e}^{ikz+\alpha t} \tag{37}$$

The same calculation as for the liquid phase leads to the final form of the profiles of the two velocity components and the pressure in the gas phase. The equations read

$$v_{r,\,\mathrm{G}} = \frac{\alpha + ik\bar{U}_{\mathrm{G}}}{K_0'(ka)}K_0'(kr)\xi_0\mathrm{e}^{ikz+\alpha t} \quad r \geq a \tag{38}$$

$$v_{z,\,\mathrm{G}} = i\frac{\alpha + ik\bar{U}_{\mathrm{G}}}{K_0'(ka)}K_0(kr)\xi_0\mathrm{e}^{ikz+\alpha t} \quad r \geq a \tag{39}$$

$$p_{\mathrm{G}} = -\frac{\rho_{\mathrm{G}}}{k}\frac{\left(\alpha + ik\bar{U}_{\mathrm{G}}\right)^2}{K_0'(ka)}K_0(kr)\xi_0\mathrm{e}^{ikz+\alpha t} \quad r \geq a \tag{40}$$

2.3. Dispersion relation

The dispersion relation of the liquid jet of a non-Newtonian fluid is derived using the normal stress boundary condition (18). The normal stress in the liquid jet can be obtained from the corresponding equations of the velocity and pressure profiles.

$$\begin{aligned}\pi_{rr} &= p + \tau_{rr} = p - 2\eta(\alpha)\frac{\partial v_r}{\partial r} \\ &= -\left\{\frac{l^2 + k^2}{I_1(ka)}\left[\frac{\rho}{k}\left(\alpha + ik\bar{U}\right)I_0(kr) + 2k\eta(\alpha)I_1'(kr)\right] - \frac{4k^2 l\eta(\alpha)}{I_1(la)}I_1'(lr)\right\}\frac{\eta(\alpha)}{\rho}\xi_0\mathrm{e}^{ikz+\alpha t}\end{aligned} \tag{41}$$

The normal stress in the gas is obtained from $\pi_{\mathrm{G},\,rr} = p_{\mathrm{G}}$

$$\pi_{\mathrm{G},\,rr} = -\frac{\rho_{\mathrm{G}}}{k}\frac{\left(\alpha + ik\bar{U}_{\mathrm{G}}\right)^2}{K_0'(ka)}K_0(kr)\xi_0\mathrm{e}^{ikz+\alpha t} \quad r \geq a \tag{42}$$

The pressure induced by the surface tension to the first order in ξ is expressed as

$$p_\sigma = \frac{\sigma}{a^2}\left(\xi + a^2\frac{\partial^2\xi}{\partial z^2}\right) = \frac{\sigma}{a^2}(1 - k^2a^2)\xi_0\mathrm{e}^{ikz+\alpha t} \tag{43}$$

Substituting the expressions found for π_{rr}, $\pi_{\mathrm{G},\,rr}$, and p_σ into the normal stress boundary condition (18) for $r = a$ yields the following dispersion relation:

$$\alpha^2\left[\frac{ka}{2}\frac{I_0(ka)}{I_1(ka)}+\frac{ka}{2}\frac{\rho_G}{\rho}\frac{K_0(ka)}{K_1(ka)}\right]+\alpha\left\{2ik\bar{U}_R\frac{ka}{2}\frac{\rho_G}{\rho}\frac{K_0(ka)}{K_1(ka)}\right.$$

$$\left.+\frac{\eta_0}{\rho a^2}\frac{1+\lambda_2(\alpha+ik\bar{U}_R)}{1+\lambda_1(\alpha+ik\bar{U}_R)}k^2a^2\left[2ka\frac{I_0(ka)}{I_1(ka)}\frac{l^2}{l^2-k^2}-1-2la\frac{I_0(la)}{I_1(la)}\frac{k^2}{l^2-k^2}\right]\right\}$$

$$=\frac{\sigma}{2\rho a^3}k^2a^2(1-k^2a^2)+\frac{\rho_G}{\rho}\frac{\bar{U}_R^2}{2a^2}k^3a^3\frac{K_0(ka)}{K_1(ka)} \tag{44}$$

Eq. (44) relates the complex frequency of a disturbance to its real wave number k. In order to solve the equation for α, it must be kept in mind that the parameter l is a function of α. For convenience and comparability with results from other authors, Eq. (44) is formulated in a coordinate system fixed with the moving jet, so that the velocities $\bar{U}$ and $\bar{U}_G$ are replaced by the relative velocity $\bar{U}_R$ between the jet and the gaseous environment.

Let us now consider a number of limiting cases of the above equation in order to verify its validity in the light of earlier theoretical work by other authors. Eq. (44) is identical to the result of Goren and Gottlieb (1982) when in their equation the axial tension is set to zero. When the gas effect is neglected (i.e., $\rho_G=0$), Eq. (44) reduces to the result obtained by Goldin et al. (1969):

$$\alpha_r^2\frac{ka}{2}\frac{I_0(ka)}{I_1(ka)}+\alpha_r\frac{\eta(\alpha)}{\rho}k^2\left[2ka\frac{I_0(ka)}{I_1(ka)}\frac{l^2}{l^2-k^2}-1-2la\frac{I_0(la)}{I_1(la)}\frac{k^2}{l^2-k^2}\right]$$

$$=\frac{\sigma k^2a^2}{2\rho a^3}(1-k^2a^2) \tag{45}$$

A comparison with the equation printed in Goldin et al. (1969) reveals a misprint on their right-hand side, where the factor 1/2 should be erased. With $\lambda_2=0$ in $\eta(\alpha)$, the dispersion relation for a jet of a Maxwell fluid emerges. When $\lambda_1=0$ and $\lambda_2=0$, the viscoelastic fluid is transformed into a Newtonian fluid (in this case $\eta_0=\mu$, where μ is the dynamic viscosity of the Newtonian fluid, and the ratio μ/ρ is denoted ν), and the dispersion equation (45) readily reduces to the result for a Newtonian fluid obtained by Weber (1931):

$$\alpha_r^2\frac{ka}{2}\frac{I_0(ka)}{I_1(ka)}+\alpha_r\nu k^2\left[2ka\frac{I_0(ka)}{I_1(ka)}\frac{l^2}{l^2-k^2}-1-2la\frac{I_0(la)}{I_1(la)}\frac{k^2}{l^2-k^2}\right]=\frac{\sigma k^2a^2}{2\rho a^3}(1-k^2a^2) \tag{46}$$

Furthermore, when the liquid viscosity vanishes, Eq. (46) readily reduces to Rayleigh's (1878) famous result for an inviscid liquid jet in a vacuum:

$$\alpha_r^2=\frac{\sigma}{\rho a^3}ka(1-k^2a^2)\frac{I_1(ka)}{I_0(ka)}. \tag{47}$$

From the above derivations it is seen that the dispersion relations for Newtonian and inviscid liquid jets with or without gas effects are recovered by the non-Newtonian liquid jet dispersion

relation (44). This equation will be tested against experimental data from the literature and analyzed in the following section.

3. Results

For convenience, the dispersion relation (44) of a non-Newtonian liquid jet may be expressed in non-dimensional form. We write down only the real part of the complex equation, since we will not consider travelling waves on the jet (i.e., we restrict to an analysis of the purely temporal instability behavior of the jet). The real dispersion relation for a jet of a viscoelastic liquid reads in non-dimensional form

$$\begin{aligned}&\Omega_r^2\frac{ka}{2}\left[\frac{I_0(ka)}{I_1(ka)}+\frac{\rho_G}{\rho}\frac{K_0(ka)}{K_1(ka)}\right]+\Omega_r k^2a^2Z\frac{Z+\tilde{\lambda}El\Omega_r}{Z+El\Omega_r}\left[2ka\frac{I_0(ka)}{I_1(ka)}\right.\\&\left.\times\left(1+k^2a^2\frac{Z}{\Omega_r}\frac{Z+\tilde{\lambda}El\Omega_r}{Z+El\Omega_r}\right)-1-2la\frac{I_0(la)}{I_1(la)}k^2a^2\frac{Z}{\Omega_r}\frac{Z+\tilde{\lambda}El\Omega_r}{Z+El\Omega_r}\right]\\&=\frac{k^2a^2}{2}(1-k^2a^2)+C\cdot\frac{\rho_G}{\rho}\frac{k^3a^3}{2}We\frac{K_0(ka)}{K_1(ka)}\end{aligned}\tag{48}$$

where $\Omega_r=\alpha_r/(\sigma/\rho a^3)^{1/2}$ is the non-dimensional growth rate, ka is the non-dimensional (real) wave number, ρ_G/ρ is the ratio of gas and liquid density, $We=\bar{U}_R^2a\rho/\sigma$ is the Weber number formed with the relative velocity $\bar{U}_R$, the jet radius and the liquid density. The symbol $\tilde{\lambda}=\lambda_2/\lambda_1$ denotes the ratio of deformation retardation to stress relaxation time (called the time constant ratio for short). The values of this quantity are regarded to lie between 1/9 and 1 by Bird et al. (1977), while Goren and Gottlieb (1982) use a value of 0.1. The Ohnesorge number Z is defined as $Z=\eta_0/(\rho\sigma a)^{1/2}$ and denotes the ratio of viscous forces to surface tension forces. A new group, the Elasticity number, appears which is defined in Kroesser and Middleman (1969) as

$$El=\frac{\eta_0\lambda_1}{\rho a^2}.\tag{49}$$

This number represents a ratio of viscous and elastic time scales of the liquid jet. The constant C in front of the aerodynamic term on the right-hand side of Eq. (48) was introduced in order to account for the correction due to Sterling and Sleicher (1975). This constant corrects empirically the action of the aerodynamic forces on the disintegrating jets in the absence of velocity profile relaxation. According to Sterling and Sleicher (1975), the value of the constant $C=0.175$. This value is used in the present calculations also, since it is caused by the aerodynamic interaction of the jet with its gaseous host medium and does not depend on the rheological behavior of the liquid. The derivation of a dispersion relation for ultrasound-modulated two-fluid atomization of liquid jets led Tsai et al. (1999) to a similar correction factor, which in their equation accounts for the fact that, when surface waves are exposed to

aerodynamic force, in general only part of the wave feels the force. The factor β they introduce into their equation in front of the aerodynamic term assumes values between 0.5 and 0.8.

Similarly, the dispersion relation of a Newtonian liquid jet can be non-dimensionalized as

$$\Omega_r^2\frac{ka}{2}\left[\frac{I_0(ka)}{I_1(ka)}+\frac{\rho_G}{\rho}\frac{K_0(ka)}{K_1(ka)}\right]+\Omega_r k^2a^2Z\left[2ka\frac{I_0(ka)}{I_1(ka)}\left(1+k^2a^2\frac{Z}{\Omega_r}\right)-1\right.$$
$$\left.-2la\frac{I_0(la)}{I_1(la)}k^2a^2\frac{Z}{\Omega_r}\right]$$
$$=\frac{k^2a^2}{2}(1-k^2a^2)+C\cdot\frac{\rho_G}{\rho}\frac{k^3a^3}{2}We\frac{K_0(ka)}{K_1(ka)} \tag{50}$$

For an inviscid liquid jet, the corresponding non-dimensional dispersion relation reads

$$\Omega_r^2\frac{ka}{2}\left[\frac{I_0(ka)}{I_1(ka)}+\frac{\rho_G}{\rho}\frac{K_0(ka)}{K_1(ka)}\right]=\frac{k^2a^2}{2}(1-k^2a^2)+C\cdot\frac{\rho_G}{\rho}\frac{k^3a^3}{2}We\frac{K_0(ka)}{K_1(ka)} \tag{51}$$

The instability of liquid jets corresponds to positive values of the disturbance growth rate (i.e., $\alpha_r > 0$ and $\Omega_r > 0$), and the growth rate of disturbances as a function of the non-dimensional wave number ka can be obtained by solving the above dispersion relations iteratively, searching the zeros in α_r or Ω_r for each given ka.

Before going into the details of an analysis of the derived dispersion relation for non-Newtonian jets, an attempt is made to compare the relation and its predictions with experiments and theories from other authors. This comparison is important, since a meaningful interpretation of the results from the present theory can only be given if the range of validity of the theory is checked. Since an essential part of the theory is the axial symmetry of the jet deformations, the onset of bending instabilities is an important issue in this context.

3.1. Comparison with results of other authors and validation of the theory

For a first comparison, computational results from the present theory are compared with the dispersion relation and measurement results for the growth rate spectrum by Gordon et al. (1973). In Fig. 13 of Gordon et al., the authors show the dispersion relation for a jet of an aqueous 0.05% Separan AP30 solution. Separan is a polyacrylamide frequently used in experiments on viscoelastic jets. The jet radius is 0.921 mm, the Ohnesorge number formed with the jet diameter is 0.305. The values of both density and surface tension of that solution are practically identical with those of water. The computed dispersion relation of Gordon et al. does not account for the action of the ambient gas. In Fig. 2, the results of Gordon et al. (1973) are shown together with the dispersion relation according to the present theory. The symbols indicate the experimental results from Gordon et al. (1973), and the dispersion relation of Gordon et al. is represented by the dashed line. The dispersion relation from the present theory is given by the solid line. The calculations with the present theory were carried out using the parameter values $a = 0.921$ mm, $\rho = 1000$ kg/m^3, $\sigma = 70 \times 10^{-3}$ N/m, $\eta_0 = 0.11$

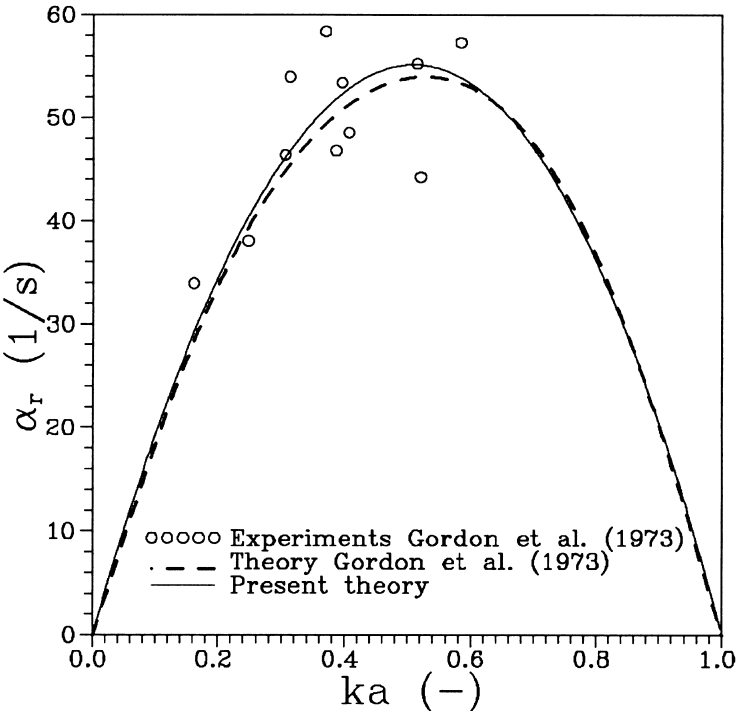

Fig. 2. The dimensional growth rate α_r of disturbances on jets of an 0.05% aqueous Separan solution as a function of the nondimensional wave number ka according to Gordon et al. (1973) and the present theory. Parameters are $\bar{U}_R = 0$, $a = 0.921$ mm, $\rho = 1000$ kg/m^3, $\sigma = 70.5 \times 10^{-3}$ N/m, $\eta_0 = 0.11$ Pa s. The viscoelastic liquid is characterized by $\lambda_1 = 0.1$ ms, $\lambda_2 = 0.01$ ms in the present theory.

Pa s. The elasticity of the liquid was characterized by the time scales $\lambda_1 = 0.1$ ms and $\lambda_2 = 0.01$ ms. From the paper of Gordon et al. (1973) no information on these time scales of the liquid could be extracted, so that the values had to be estimated. The relative jet velocity $\bar{U}_R$ was set to zero for comparison. The results reveal a good mutual agreement of the two dispersion relations and the measurements. However, it should be noted that in this calculation the parameters λ_1 and λ_2 play the role of adjustable parameters, since any information about the Separan solution in this respect was missing. Nonetheless, the present theory reproduces the results by Gordon et al. excellently.

Another comparison is drawn with the results of Kroesser and Middleman (1969). Fig. 2 of their paper depicts the measured non-dimensional breakup length $L/2a$ of (Newtonian and) viscoelastic jets as a function of $\sqrt{We}\,(1 + 3Z)$. The viscoelastic liquid used in the experiments was a 3.78% solution of the polymer L100 (a PIB with the molecular weight of 7.3×10^5) in Tetralin, with the density 970 kg/m^3, the surface tension 29×10^{-3} N/m, and the zero shear viscosity 0.2 Pa s. The relaxation time $\lambda_1 = 2.1$ ms of the liquid was calculated using the Bueche theory (Bueche, 1954). The Weber number $We = \bar{U}_R^2 a\rho/\sigma$ of the data points varies between 2.87 and 2866, the non-dimensional breakup lengths lie between 47 and 1877. The breakup lengths were calculated by Kroesser and Middleman using their theory which yields the equation

$$\frac{L}{2a} = C_1 \cdot \sqrt{We}\,(1+3Z), \tag{52}$$

where the coefficient C_1 is a function of the Weber and Elasticity numbers of the form

$$C_1 = \frac{C_2}{1+3El/(1+3Z)^2} \tag{53}$$

and the coefficient C_2 is claimed to assume values between 12 and 13, as the analogous coefficient in Weber's equation for Newtonian liquids (Haenlein, 1931). An inspection of the data in the paper, however, shows that this is not the case and C_2 is not constant. Using the values of C_1 given in Fig. 4 of Kroesser and Middleman (1969), the non-dimensional breakup lengths $L/2a$ were calculated using the maximum wave growth rate α^* from the present theory in the equation

$$\frac{L}{2a} = C_1 \cdot \frac{U}{2a\alpha^*} \tag{54}$$

The comparison of the results with the data of Fig. 2 in Kroesser and Middleman (1969) is given in Fig. 3. The figure shows that the present linearized stability analysis reproduces the

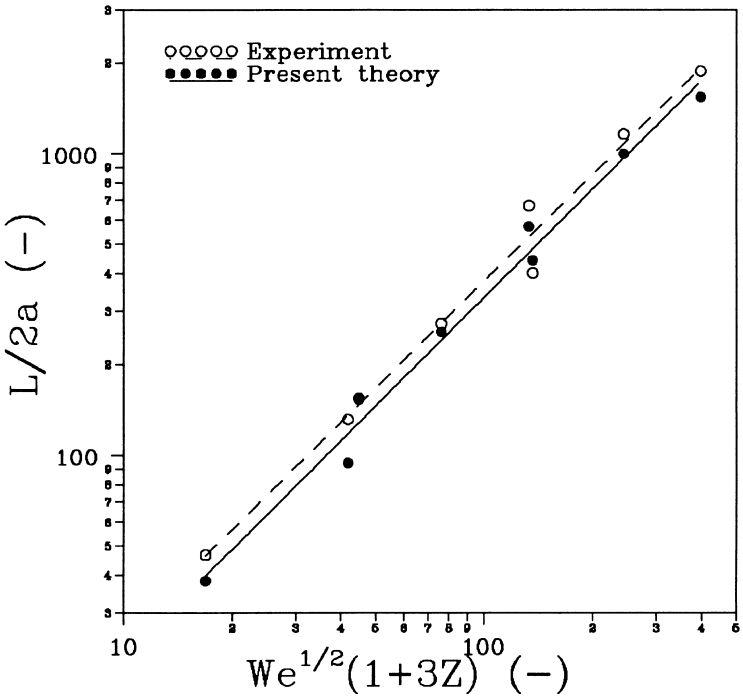

Fig. 3. The nondimensional breakup length of 3.78% L100/Tetralin jets as a function of $We^{1/2}(1+3Z)$ according to Kroesser and Middleman (1969) experiments and the present theory. The jet velocity varies between 0.73 and 16.4 m/s. The jet radius assumes values of 0.15, 0.205 and 0.31 mm, the liquid density $\rho = 970$ kg/m^3, $\rho_G = 1.2$ kg/m^3, $\sigma = 29 \times 10^{-3}$ N/m, $\eta_0 = 0.2$ Pa s. The viscoelastic liquid is characterized by $\lambda_1 = 2.1$ ms, $\lambda_2 = 0.21$ ms.

results very accurately, but yields systematically shorter breakup lengths than the work by Kroesser and Middleman. The reason for the good agreement is the fact that the set of coefficients C_1 given in Fig. 4 of Kroesser and Middleman (1969) was calculated by these authors such that their theory describes the experimental behavior of the jets accurately. Since the theory by Kroesser and Middleman does not account for aerodynamic influence on the jet, it is quite obvious that the comparison with the present theory must lead to the observed smaller breakup lengths. The average deviation between the two sets of results is 14%. With these results, however, it is not possible to estimate a limitation of applicability of a linear theory.

Goldin et al. (1969) provide results of measurements on the breakup lengths of jets of aqueous Separan solutions at different concentrations for varying jet velocity. The results for a 0.05% solution are shown in Fig. 4 in comparison with calculated values from the present theory obtained using Eq. (54) with the value $C_1 = 12$. For calculating the maximum growth rate α^* from the present theory, the same values of λ_1 and λ_2 were used as for the above comparison with the paper by Gordon et al. (1973). Fig. 4 clearly shows that the present theory underestimates the measured breakup lengths at small Weber numbers considerably, while it may even overestimate the breakup length for large Weber numbers, where the breakup length has become independent of the Weber number. It is therefore virtually impossible to calculate breakup lengths of viscoelastic jets with the present theory. The obvious

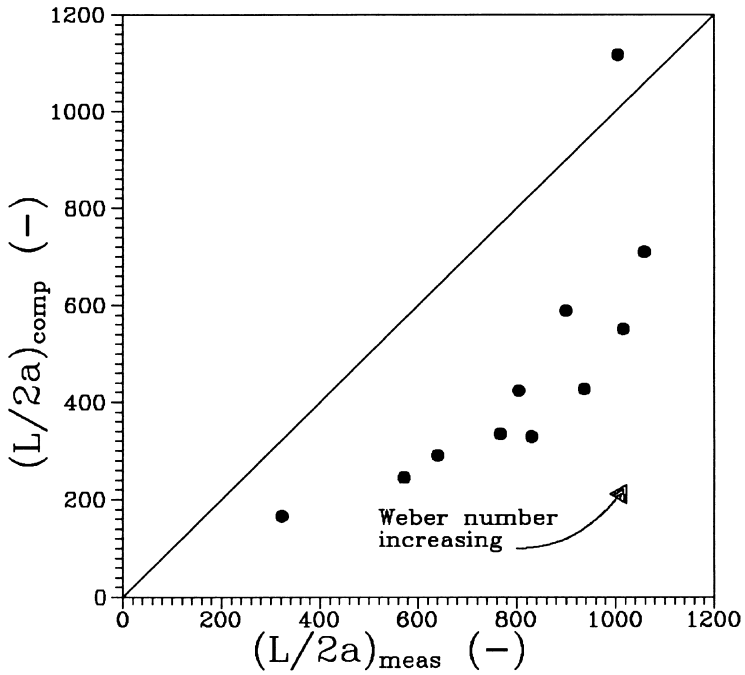

Fig. 4. The nondimensional breakup length of 0.05% aqueous Separan solution jets according to measurements by Goldin et al. (1969) in comparison with computational results from the present theory ($\bar{U}_R$ varying between 2.15 and 14.7 m/s, a varying between 0.1315 and 0.434 mm, $\rho = 10^3$ kg/m^3, $\rho_G = 1.2$ kg/m^3, $\sigma = 70 \times 10^{-3}$ N/m, $\eta_0 = 0.11$ Pa s, $\lambda_1 = 0.1$ ms, $\lambda_2 = 0.01$ ms).

reason is the strong influence of nonlinear retardation in the late stages of the breakup which is not accounted for in linear theories.

Another aspect of the applicability of the present theory is the onset of bending instability of the jets, as quantified by Yarin (1993). Since the present theory accounts only for symmetric jet deformations, it must be made sure that the jet parameters treated with the theory ensure the absence of bending instabilities. Yarin (1993) derives a dispersion relation between the growth rate γ of bending instabilities on liquid jets and the wave number $\chi = 2\pi a/l$ formed with the wavelength l of the disturbances. The dispersion relation formulated for a Maxwell fluid in Yarin (1993) reads

$$\gamma^2 + \frac{3}{4}\frac{\chi^4}{\rho a^2}\frac{\mu}{1+\gamma\lambda_1}\cdot\gamma + \chi^2\left(\frac{\sigma}{\rho a^3} - \frac{\rho_G}{\rho}\frac{\bar{U}_R^2}{a^2} + \frac{T_{zz}}{\rho a^2}\right) = 0, \tag{55}$$

where the axial tension T_{zz} acts as a stabilizing factor. The dispersion relation (55) yields positive values of the growth rate γ of the bending instabilities only when the third term on the left-hand side is negative. This leads to the instability criterion

$$We > \frac{\rho}{\rho_G}(1+Te), \tag{56}$$

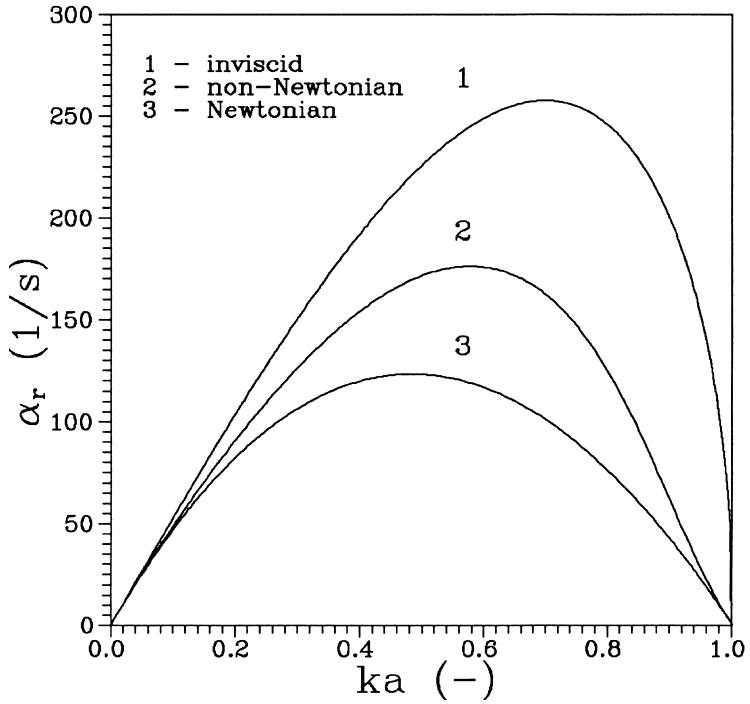

Fig. 5. The dimensional growth rate α_r of disturbances on different liquid jets versus the non-dimensional wave number ka at $\bar{U}_R = 2$ m/s, $a = 0.5$ mm, $\rho = 1000$ kg/m^3, $\rho_G = 1.2$ kg/m^3, $\sigma = 70 \times 10^{-3}$ N/m, $\eta_0 = 0.1$ Pa s. The viscoelastic liquid is characterized by $\lambda_1 = 10$ ms, $\lambda_2 = 1$ ms.

where the non-dimensional tension group $Te = T_{zz}a/\sigma$ (as defined in Goren and Gottlieb, 1982) and the Weber number is formed with the relative jet velocity $\bar{U}_R$ and the jet radius a. This onset criterion (56) for bending instabilities shows the stabilizing effect of axial tension in the liquid.

Under the assumption that the axial tension is fully relaxed, relation (56) leads to an onset Weber number for bending instabilities of the order of 10^3 for liquids in an atmospheric environment. This means that the data of Kroesser and Middleman (1969) for the higher Weber numbers (of up to 2866) cannot be treated with theories based on axisymmetric jet deformations. This is part of the reason for the strongly varying coefficients C_1 introduced by Kroesser and Middleman (1969). In order to verify the result of the onset criterion (56), photographs of disintegrating jets as presented in Figs. 5–9 of the paper by Goldin et al. (1969) were inspected. The liquids used in these experiments were — among others — aqueous solutions of the elastic polymers Separan AP30, Guar gum and Sodium Carboxy-Methyl Cellulose (SCMC) at different concentrations. The photographs show typical growth of symmetrical waves on the jets at small Weber numbers around 130. Sinusoidal waves with large, growing amplitudes are seen in Fig. 9a of that paper, where a 0.25% Separan jet at a Weber number of 1218 and an Ohnesorge number of 11.5 is shown. Such waves are visible on the jet in Fig. 9d–i of the paper also, which depict a jet at a Weber number of 295. However,

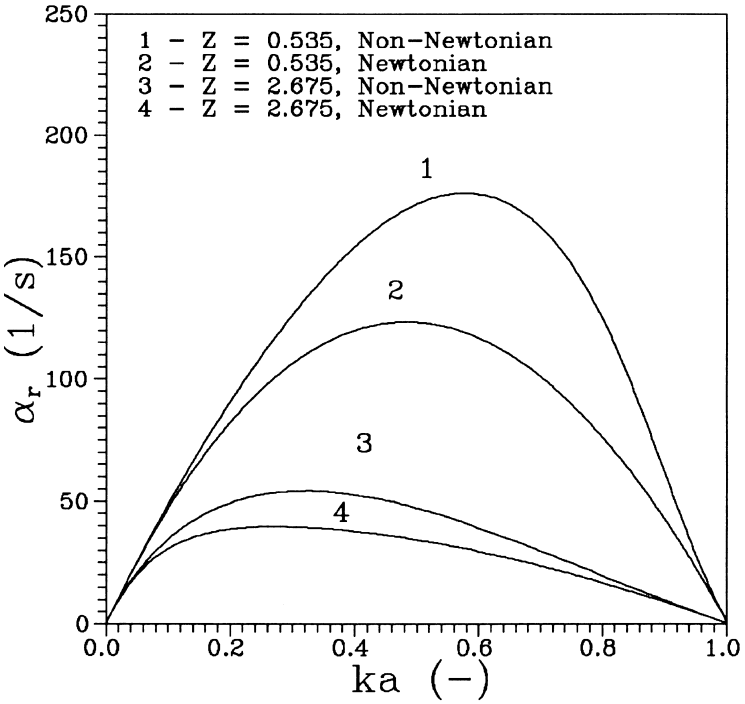

Fig. 6. Effects of the Ohnesorge number on the dimensional growth rate α_r of disturbances on non-Newtonian and Newtonian liquid jets versus the non-dimensional wave number ka at $We = 28.6$, $El = 4$, $\lambda_1 = 10$ ms, $\lambda_2 = 1$ ms. The viscosity η_0 varies between 0.1 and 0.5 Pa s.

with this small Weber number, the sinusoidal waves do not grow. These observations confirm the conclusion that only Weber numbers below $O(10^3)$ may be treated with the present theory.

3.2. Analysis of the dispersion relation

Having checked the applicability of the present theory to disintegrating liquid jets of viscoelastic liquids at sufficiently small Weber numbers, we undertake an analysis of the predictions on the growth rate spectra derived from the theory. Fig. 5 shows the dimensional growth rate α_r of axisymmetrical disturbance waves on different liquid jets as a function of the non-dimensional wave number ka for $\bar{U}_R = 2$ m/s, $a = 0.5$ mm, $\rho = 10^3$ kg/m^3, $\rho_G = 1.2$ kg/m^3, and $\sigma = 70 \times 10^{-3}$ N/m. The zero shear viscosity η_0, i.e. for the Newtonian fluid the dynamic viscosity, is 0.1 Pa s. The time scales of the viscoelastic fluid are $\lambda_1 = 10$ ms and $\lambda_2 = 1$ ms. This data set corresponds to the non-dimensional numbers $We = 28.6$, $Z = 0.535$, and $El = 4$. In Fig. 5, curve 1 represents the inviscid, curve 2 the non-Newtonian, and curve 3 the Newtonian fluid. The figure shows that the growth rate of disturbances on a non-Newtonian liquid jet is larger than that for a Newtonian and smaller than that for an inviscid fluid. Therefore, it is concluded that, in the range of flow parameters associated with the results of Fig. 5, a jet of a non-Newtonian fluid is more unstable than a Newtonian liquid jet. This is not surprising, since, while Newtonian jets appear rigid, viscoelastic jets have the additional elastic

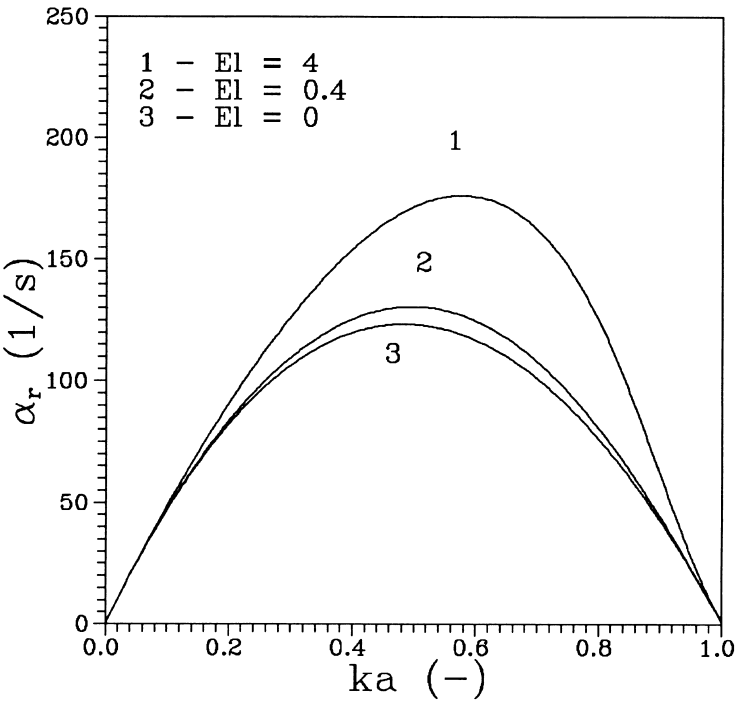

Fig. 7. Effects of the Elasticity number on the dimensional growth rate α_r of disturbances on non-Newtonian liquid jets versus the non-dimensional wave number ka at $We = 28.6$, $Z = 0.5345$, $\tilde{\lambda} = 0.1$ (with $\lambda_1 = 10$ ms), $\rho = 1000$ kg/m^3, $\rho_G = 1.2$ kg/m^3.

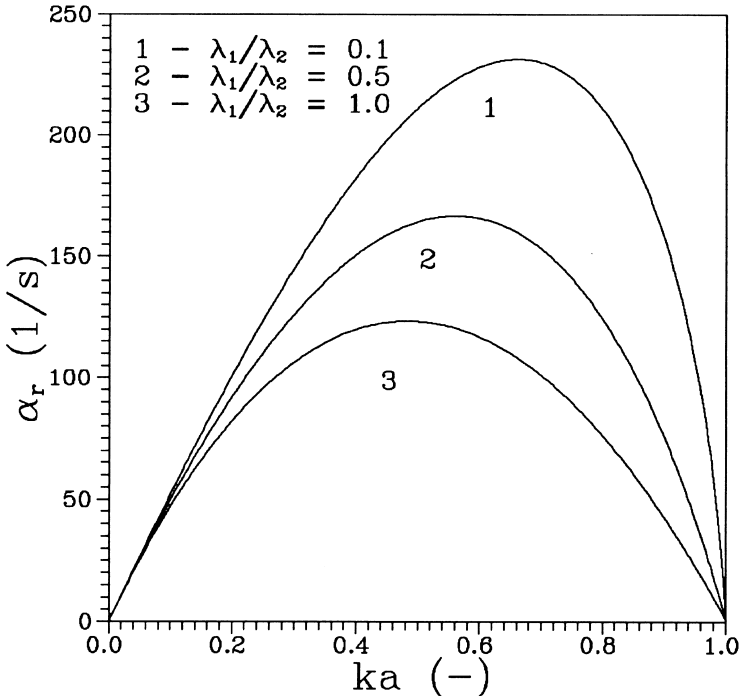

Fig. 8. Effects of the time constant ratio on the dimensional growth rate α_r of disturbances on non-Newtonian liquid jets versus the non-dimensional wave number ka at $We = 28.6$, $Z = 0.535$, $El = 0.4$ (with $\lambda_1 = 1$ ms), $\rho = 1000$ kg/m^3, $\rho_G = 1.2$ kg/m^3.

freedom for deformation. Similar results were reported by Goldin et al. (1969). It is inferred that any experimentally observed difference in the breakup behavior of liquid jets must, therefore, be due to nonlinear phenomena. Goldin et al. (1969) came to the same conclusion.

The cutoff wave number is the value of the wave number where the growth rate curve crosses the wave number axis in the plot of wave growth rate versus wave number, and it is obtained from the dispersion relations by setting $\alpha_r = 0$ or $\Omega_r = 0$. The liquid jet is stable against disturbances with wave numbers above the cutoff wave number. Only those disturbances with wave numbers lower than the cutoff wave number are unstable. In this sense, the range left to the cutoff wave number can be called the instability range of the liquid jet, and the area under the growth rate curve of the jet in the plot of the dispersion relation may be called the instability region.

From inspection of dispersion relations (50) and (51), it is evident that for Newtonian fluids, the Ohnesorge number appears in dispersion relation (50) due to the presence of liquid viscosity effects. It is clear that, when the Ohnesorge number is nonzero, to balance dispersion relation (50) for given conditions, the growth rate must decrease accordingly, as compared to an inviscid fluid described by Eq. (51). This analysis is confirmed by the results shown in Fig. 5. Furthermore, as the Ohnesorge number is increased, the growth rate decreases. Therefore, it is concluded that the area between the growth rate curve of the inviscid liquid jet and that of the Newtonian counterpart is caused by the liquid viscosity effects, and in this sense, this area can

be termed the viscosity-induced region. The size of this area depends on the value of the liquid viscosity.

For non-Newtonian fluids, it can be seen from dispersion relation (48) that a term with the Elasticity number is introduced due to the liquid elasticity effects, and it is clear that the term $(Z+\tilde{\lambda}El\Omega_r)/(Z+El\Omega_r)$ is less than one. Thus, compared with the dispersion relation for Newtonian fluids, the corresponding non-dimensional growth rate of a non-Newtonian jet must increase to balance the equations for given conditions. From further inspection of the term $(Z+\tilde{\lambda}El\Omega_r)/(Z+El\Omega_r)$, it is inferred that an increase of the time constant ratio or a decrease of the Elasticity number El leads to a decrease of the growth rate, which is easy to confirm by evaluating Eq. (48). In summary, for non-Newtonian fluids, both viscosity and elasticity effects exist at the same time, which makes the instability behavior more complicated than for Newtonian fluids. In general, the liquid viscosity tends to stabilize the jet in comparison with inviscid fluids by decreasing the disturbance growth rate, whereas the liquid elasticity results in a destabilization. Under the common action of both the liquid viscosity and the elasticity effects, the growth rate curve of non-Newtonian liquid jets lies between those of inviscid and Newtonian ones, as shown by the results in Fig. 5. On the basis of this discussion, it is believed that the area between the growth rate curves of the inviscid and non-Newtonian liquid jets is induced by the interaction of the liquid viscosity and elasticity effects in the non-Newtonian fluid. In this sense, this area is called the viscoelasticity-induced region, and the area between

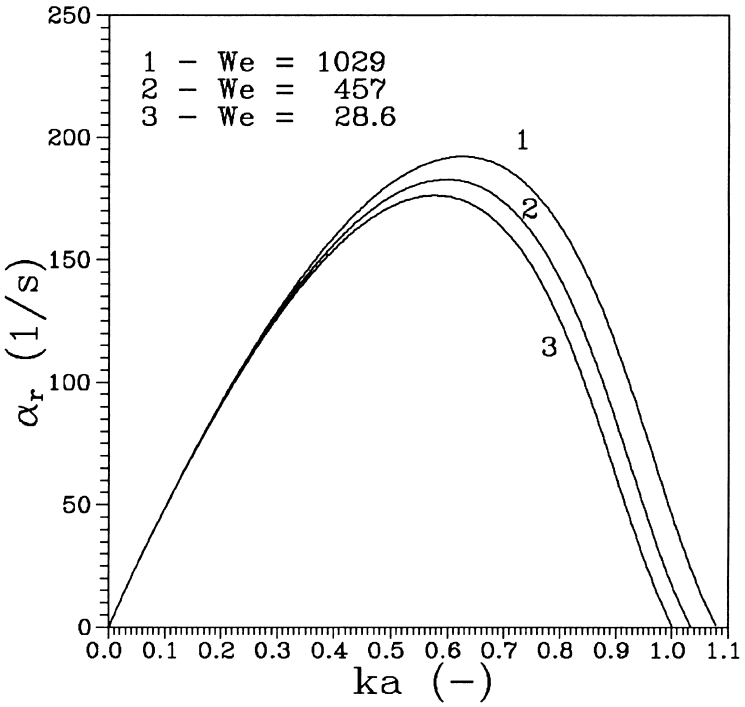

Fig. 9. Effects of the liquid Weber number on the dimensional growth rate α_r of disturbances on non-Newtonian liquid jets versus the non-dimensional wave number ka at $Z=0.535$, $El=4$, $\rho=1000$ kg/m^3, $\rho_G=1.2$ kg/m^3, $\lambda_1=10$ ms, and $\lambda_2=1$ ms.

the growth rate curves of the Newtonian and non-Newtonian liquid jets is termed the elasticity-induced region.

The effects of the liquid viscosity, through the Ohnesorge number Z, on the growth rate of Newtonian and non-Newtonian liquid jets are displayed in Fig. 6, where the Ohnesorge number is increased from 0.535 to 2.675, while the other flow parameters are held at $We = 28.6$, $El = 4$ with the same values of the characteristic times λ_1 and λ_2 for the two non-Newtonian fluids shown. It is seen from Fig. 6 that, as the Ohnesorge number is increased fivefold, the values of the growth rate of disturbances are reduced drastically as a result of the increased liquid viscosity. For each Ohnesorge number, however, the non-Newtonian fluid exhibits larger growth rates of disturbances, i.e., it is less stable than the Newtonian counterpart. The reason for this fact has been discussed above. However, the instability range does not change with the Ohnesorge number. In addition, it can be concluded from Fig. 6 that, as the Ohnesorge number is increased, the growth rate curve of the non-Newtonian liquid jet approaches that of the Newtonian one, since the damping effect of the high viscosity overwhelms the elastic effects.

In order to explore the effects of the liquid elasticity on the evolution of axisymmetric disturbances of non-Newtonian liquid jets, the Elasticity number El was varied between 4.0

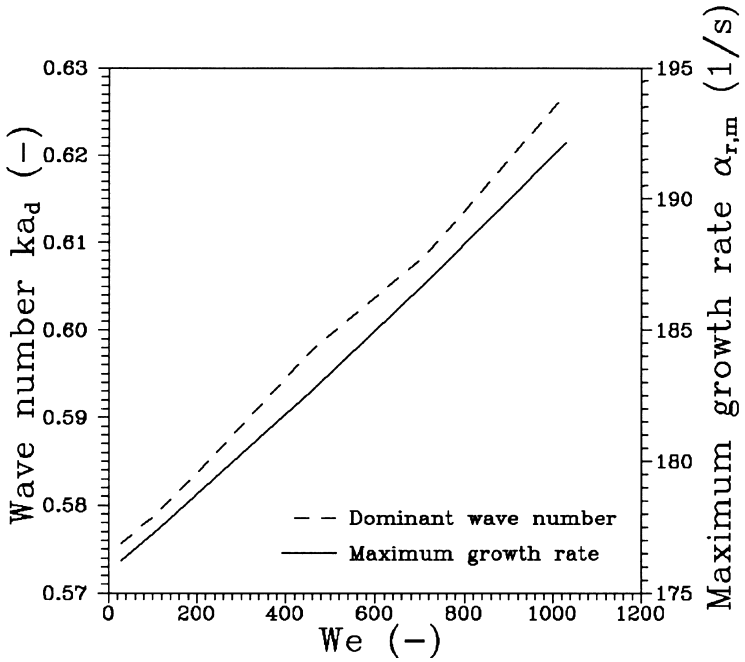

Fig. 10. Effects of the liquid Weber number on the dimensional maximum growth rate $\alpha_{r,m}$ and the non-dimensional dominant wave number ka_d of disturbances on non-Newtonian liquid jets at $Z = 0.535$, $El = 4$, $\rho = 1000$ kg/m^3, $\rho_G = 1.2$ kg/m^3, $\lambda_1 = 10$ ms, and $\lambda_2 = 1$ ms.

and 0, while the other parameters were kept at $We = 28.6$, $Z = 0.535$, and $\tilde{\lambda} = 0.1$. The results are shown in Fig. 7. It is observed that, despite the varying liquid elasticity, the growth rates of disturbance waves remain almost identical in the long-wave range $ka \leq 0.1$. At higher values of the wave number, the growth rates of waves decrease with the reduction of the liquid elasticity. When the Elasticity number is equal to zero, the non-Newtonian fluid is transformed into a Newtonian one. Therefore, it is concluded that increasing liquid elasticity tends to increase the growth rate of waves on non-Newtonian liquid jets. Thus, it is further confirmed that the linearized computations predict the non-Newtonian liquid jets to be more unstable than Newtonian ones for the conditions given here. In addition, the cutoff wave number remains unchanged, despite the variation of the Elasticity number.

As a next step, the influence of the ratio $\tilde{\lambda}$ of deformation retardation to stress relaxation time on the growth rate of waves on non-Newtonian liquid jets was analyzed. The computational results for varying time constant ratio between 0.1 and 1 are presented in Fig. 8. The Weber number $We = 28.6$, the Ohnesorge number was kept at $Z = 0.535$, the Elasticity number $El = 0.4$, with $\lambda_1 = 1$ ms. Fig. 8 indicates that, as the time constant ratio is increased, the growth rates of disturbances stay almost identical for wave numbers less than 0.08, but decrease at higher values of the wave number. Moreover, it is obvious from Fig. 8 that the instability range does not change with varying time constant ratio. It is clear from a

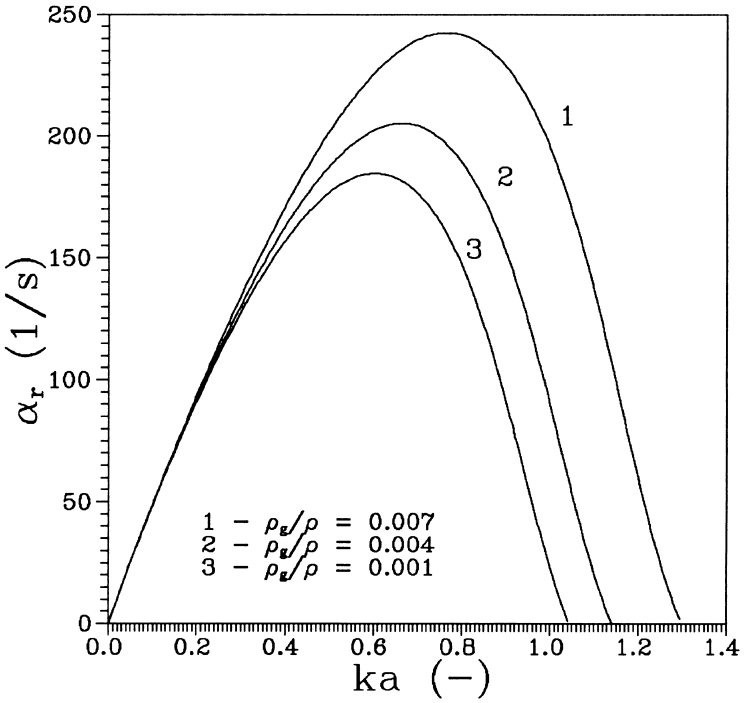

Fig. 11. Effects of the gas-to-liquid density ratio on the dimensional growth rate α_r of disturbances on non-Newtonian liquid jets versus the non-dimensional wave number ka at $We = 578$, $Z = 0.535$, $El = 4$, $\rho = 1000$ kg/m^3, $\rho_G = 1.2$ kg/m^3, $\lambda_1 = 10$ ms, and $\lambda_2 = 1$ ms.

comparison between Figs. 7 and 8 that the effects of the time constant ratio on the growth rate are similar to those of the Elasticity number, but the trends of changes are opposite.

Fig. 9 shows the effects of the liquid Weber number We on the growth rate of disturbance waves on non-Newtonian liquid jets at $Z = 0.535$, $El = 4$ and $\tilde{\lambda} = 0.1$. In Fig. 9, the liquid Weber number We is varied from 28.6 to 1029. From inspection of Fig. 9, it is obvious that both the growth rate and the instability range increase substantially, as the liquid Weber number is increased, indicating that, e.g., an increase of the jet velocity destabilizes the non-Newtonian liquid jets. The surface tension resists the onset and development of short-wave instability on non-Newtonian liquid jets, i.e., it smoothes out the disturbances on the interface between the liquid and the gas. Reitz (1978) and Lefebvre (1989) reported a similar conclusion in their instability analyses of Newtonian liquid jets.

In Fig. 10 the effects of the liquid Weber number on the maximum growth rate and the dominant wave number of disturbances on non-Newtonian liquid jets are depicted at conditions corresponding to Fig. 9. As the liquid Weber number is increased, the maximum growth rate and the dominant wave number increase substantially, indicating that non-Newtonian liquid jets destabilize more easily at high values of the liquid Weber number for the given conditions. An increase of the Weber number may be caused either by an increase of the jet velocity, radius or density, or by decreasing surface tension.

The effects of the gas-to-liquid density ratio on the disturbance growth rates are examined in Fig. 11 at $We = 578$, $Z = 0.535$, $El = 4$, and $\tilde{\lambda} = 0.1$. It is observed that the trends discussed in relation with Fig. 9 are continued to be seen in Fig. 11. Increasing the gas-to-liquid density ratio leads to increased growth rates and cutoff wave numbers, as manifested in Fig. 11. This indicates that an increase in the ambient gas density leads to an enhancement of instability on non-Newtonian liquid jets, which means that a high ambient gas density, such as in the combustion chamber of a Diesel engine, enhances the liquid fuel atomization. It is obvious from Fig. 11 that the dominant wave number increases with increasing ratio ρ_G/ρ since the aerodynamic effects, which tend to decrease the dominant wavelengths, have increased.

4. Conclusions

The temporal instability behavior of non-Newtonian liquid jets moving in an inviscid gaseous environment was investigated for axisymmetrical disturbances. The results are summarized as follows.

1. From linearized equations of motion and the constitutive equation of the non-Newtonian fluid, a dispersion relation for axisymmetric disturbances on a non-Newtonian liquid jet was derived. This linear theory was shown to describe accurately the growth rate spectra of viscoelastic liquid jets measured in experiments by other authors. At the same time, in contrast to the analogous theory for Newtonian jets, the theory proves inapplicable for calculating the breakup lengths of viscoelastic jets. The reason is the strong influence of nonlinear processes during the final stages of viscoelastic jet breakup, which lead to the formation of beads-on-string structures and strongly retard the breakup. This phenomenon is not accounted for by linear theories.

2. An evaluation of the dispersion relation for bending instabilities derived by Yarin (1993) showed that, at jet Weber numbers larger than a threshold value, sinusoidal waves start to develop and grow. Therefore, for such large Weber numbers, the presently treated axisymmetric disturbances have minor importance. The analysis of the presently derived dispersion relation was therefore carried out for Weber numbers below the threshold.

The analysis of the derived dispersion relation yielded the following results.

3. In the regime of small deformations, a jet of a viscoelastic fluid exhibits a larger growth rate of axisymmetric surface waves than a jet of a Newtonian fluid for the same Ohnesorge number, indicating that this kind of non-Newtonian liquid jets is more unstable than the corresponding Newtonian ones. This result has been obtained by other authors before.
4. An increase of the liquid viscosity dampens disturbance waves on non-Newtonian liquid jets drastically, but the cutoff wave number remains unchanged. At high liquid viscosity, the growth rate of non-Newtonian liquid jets is close to that of Newtonian ones.
5. Increasing Elasticity number and decreasing time constant ratio $\tilde{\lambda}$ lead to increased maximum growth rates of axisymmetrical disturbances on the jets.
6. Increasing surface tension resists the development of axisymmetrical instabilities on non-Newtonian liquid jets, i.e., it smoothes out disturbances on the interface between the liquid and the gas. Increasing relative velocity between the jet and the ambient gas is the source of increased growth rates of instabilities. With increasing jet velocity, the dominant wave number increases. Similar results were obtained for inviscid and Newtonian liquid jets by many other authors before.
7. An increase of the ratio of gas-to-liquid density or of the Weber number enhance both the growth rate and the instability range of non-Newtonian liquid jets for the conditions investigated here, indicating that a high-density environment leads to an enhancement of instability.

Acknowledgements

The financial support from the Deutsche Forschungsgemeinschaft through the guest professorship Er 16/109-1, which made the stay of Z.B. Liu at Erlangen University possible, is gratefully acknowledged.

References

Bird, R.B., Armstrong, R.C., Hassager, O., 1977. Dynamics of Polymeric Liquids. Volume 1: Fluid Mechanics. Wiley, New York.

Bogy, D.B., 1979. Drop formation in a circular liquid jet. Ann. Rev. Fluid Mech 11, 207–228.

Bueche, F., 1954. J. Chem. Phys 22, 603 cited in Kroesser and Middleman (1969).

Chigier, N.A., Reitz, R.D., 1996. Regimes of jet breakup and breakup mechanisms. Progress in Astronautics and Aeronautics 1, 109–136.

Goedde, E.F., Yuen, M.C., 1970. Experiments on liquid jet instability. J. Fluid Mech 40, 495–512.

Goldin, M., Yerushalmi, J., Pfeffer, R., Shinnar, R., 1969. Breakup of a laminar capillary jet of a viscoelastic fluid. J. Fluid Mech 38, 689–711.

Gordon, M., Yerushalmi, J., Shinnar, R., 1973. Instability of jets of non-Newtonian fluids. Trans. Soc. Rheol 17, 303–324.

Goren, S., Gottlieb, M., 1982. Surface-tension-driven breakup of viscoelastic liquid threads. J. Fluid Mech 120, 245–266.

Grant, R.P., Middleman, S., 1966. Newtonian jet stability. AIChE J 12, 669–678.

Haenlein, A., 1931. Über den Zerfall eines Flüssigkeitsstrahles. Forschung auf dem Gebiete des Ingenieurwesens 2, 139–149.

Kroesser, F.W., Middleman, S., 1969. Viscoelastic jet stability. AIChE J 15, 383–386.

Lefebvre, A.H., 1989. Atomization and Sprays. Hemisphere, New York.

Levich, V.G., 1962. Physicochemical Hydrodynamics. Prentice-Hall, Englewood Cliffs.

Li, X., 1995. Mechanism of atomization of a liquid jet. Atomization and Sprays 5, 89–105.

Liu, Z., Brenn, G., Durst, F., 1998. Linear analysis of the instability of two-dimensional non-Newtonian liquid sheets. J. Non-Newtonian Fluid Mech 78, 133–143.

McCarthy, M.J., Molloy, N.A., 1974. Review of stability of liquid jets and the influence of nozzle design. Chem. Eng. J 7, 1–20.

Middleman, S., 1965. Stability of a viscoelastic jet. Chem. Engng. Sci 20, 1037–1040.

Park, H.M., Lee, H.S., 1995. Nonlinear hydrodynamic stability of viscoelastic fluids heated from below. J. Non-Newtonian Fluid Mech 60, 1–26.

Phinney, R.E., 1973. Stability of a laminar viscous jet. The influence of an ambient gas. Phys. Fluids 16, 193–196.

Rayleigh, L., 1878. On the instability of jets. Proc. Lond. Math. Soc 10, 4–13.

Rayleigh, L., 1879. On the capillary phenomena of jets. Proc. Roy. Soc. London A 29, 71–97.

Rayleigh, L., 1892. On the instability of a cylinder of viscous liquid under capillary force. Phil. Mag 34, 145–154.

Reitz, R.D., 1978. Atomization and other breakup regimes of a liquid jet. Ph.D. Thesis, Princeton University.

Sterling, A.M., Sleicher, C.A., 1975. The instability of capillary jets. J. Fluid Mech 68, 477–495.

Tomotika, S., 1935. On the instability of a cylindrical thread of a viscous liquid surrounded by another viscous liquid. Proc. Roy. Soc. London A 150, 322.

Tsai, S.C., Luu, P., Tam, P., Roski, G., Tsai, C.S., 1999. Flow visualization of Taylor-mode breakup of a viscous liquid jet. Phys. Fluids 11, 1331–1341.

Weber, C., 1931. Zum Zerfall eines Flüssigkeitsstrahles. Z. Angew Math. Mech 11, 136–154.

Yarin, A.L., 1993. Free Liquid Jets and Films: Hydrodynamics and Rheology. Wiley, New York.

Yuen, M.C., 1968. Nonlinear capillary instability of a liquid jet. J. Fluid Mech 33, 151–163.